Eqs. (1), (7), and (8) into Eq. (16) to find $\lambda(\eta)$, and using this together with Eqs. (14) and (15), one can derive an equation for η_c. After η_c is determined, the velocity is calculated using Eq. (7), which in turn is used to calculate critical Reynolds number from Eq. (17). This procedure must be done numerically and iteratively. However, the computational effort is minimal.

Results and Conclusions

The results presented are a comparison of $Re^*_{\delta\,\text{critical}}$ obtained from our approximate analysis, and an exact analysis.[5] However, the exact analysis consists of an exact boundary-layer calculation in conjunction with the modified Dunn-Lin approximation and an accurate numerical procedure for satisfying the condition expressed by Eq. (14). Therefore, the comparison measures the accuracy of the simplified boundary-layer analysis, the series representation of velocity profile, and the series solution of Eq. (14).

Table 1 shows the accuracy of the approximate analysis of constant surface temperature. The difference between the two results is less than 17%. These inaccuracies can be reduced by refining the temperature profile in the heat transfer calculation.

Also shown in Table 1 is the comparison of results for variable surface temperature. In general, the approximate method provides accurate results; the maximum error does not exceed 30%. More detailed results and comparisons are presented in Ref. 4.

In conclusion, we would like to emphasize the goals and the accomplishments of the study. The study focused on developing a simple, accurate method for calculating critical Reynolds number. Up to now, no such an analysis existed. The principal results demonstrated that the present analysis can be used to accurately estimate critical Reynolds number on a flat plate for a variety of surface temperature distributions without the aid of a computer. The method requires the numerical solution of one algebraic equation; all other relationships are given in closed form. Since computational time and effort are trivial, and the majority of the relationships are given in closed form, the integration of this scheme into an eleborate low drag system design procedure appears desirable and feasible. After the effects of pressure gradients have been incorporated, the method is well-suited for drag optimization studies.

Acknowledgments

The author would like to acknowledge the suggestions and ideas given by his colleagues, Drs. J. Aroesty and C. Gazley, Jr., and a special thanks to C. D. Harris.

References

[1] Zien, Tse-Fou, "A New Integral Calculation of Skin Friction on a Porous Plate," *AIAA Journal*, Vol. 9, Sept. 1971, pp. 1423-1425.

[2] Zien, Tse-Fou, "Approximate Analysis of Heat Transfer in Transpired Boundary Layers with Effects of Prandtl Number," *International Journal of Heat and Mass Transfer*, Vol. 19, May 1976, pp. 513-521.

[3] Aroesty, J., King, W. S., Harpole, G. W., Matyskiela, W., Wazzan, A. R., and Gazley, C., Jr., "Simple Relations for the Stability of Heated and Laminar Boundary Layers in Water: Modified Dunn-Lin Method," The Rand Corporation, Santa Monica, Calif., R-2209-ARPA, March 1978.

[4] King, W. S., "An Approximate Method for Estimating the Critical Reynolds Number for a Heated Flat Plate in Water," The Rand Corporation, Santa Monica, Calif., P-6176, Aug. 1978.

[5] Harpole, G. M., "Effects of Variation in Surface Temperature," talk presented at ONR-DARPA Transition Workshop, Naval Underwater Center, San Diego, Calif., Feb. 24-25, 1977.

Calculation of Flow in the Tail Region of a Body of Revolution

Edward W. Geller
Flow Research Company, Kent, Wash.

Introduction

THE drag of a body of revolution in an incompressible viscous fluid is generally calculated with either the formula of Young[1] or Granville.[2] These formulas require velocity profile shape and momentum parameters at the tail which, for low fineness ratio bodies, are not adequately evaluated using classical boundary-layer theory (see Patel and Guven[3]). This deficiency of boundary-layer analysis motivated a search for a more accurate method for calculating aft body turbulent flow.

The primary approximation used for the resulting method is the neglect of viscous and Reynolds stresses in the rotational flow layer, except for a thin region next to the surface. For airfoils, this approximation is justified near the trailing edge by the rational asymptotic theory of Melnik and Chow.[4] The outer layer in their triple deck model is treated as inviscid and rotational. For bodies of revolution, another justification for neglecting shear stress exists. The contraction of vortex filaments provides a mechanism for vorticity change which dominates the change due to shear stress. A secondary approximation used is equating the vorticity to the reciprocal slope of the velocity profile, a common practice for shear layers with small streamline curvature. The approximation is not essential, since computational methods exist for solution without its introduction.

In the following, the region where the flow is considered to be rotational but without shear stress will be called the calculation region. Surrounding regions are the upstream boundary layer, outer potential flow, and inner viscous surface layer. The boundary conditions for the calculation region can be obtained by an iterative match to the flow calculations for these other regions. Our investigation, however, did not attempt this more extensive problem of computing the entire flowfield; in order to check the calculation method, experimentally measured boundary conditions were used for the outer and upstream borders. The flow was matched to an inner viscous surface layer calculation in a very rudimentary sense by assuming a shape for the velocity profile in that layer.

The Dominant Vorticity Change Mechanism

Consider the material derivative of the vorticity ω

$$\frac{D\omega}{Dt} = \omega \cdot \nabla v + \nu \nabla^2 \omega \qquad (1)$$

The first term is associated with vortex filament stretching in the velocity field v, and shear stress is the mechanism responsible for the second term. For laminar flow, ν is the kinematic viscosity. For turbulent flow, consider ν to be an analogous parameter associated with the Reynolds stress.

For axisymmetric flow with axial and radial coordinates x

Received Feb. 20, 1979; revision received July 12, 1979.

Index categories: Boundary Layers and Convective Heat Transfer—Turbulent; Computational Methods; Hydrodynamics.

*Research Scientist. Member AIAA.

and r, Eq. (1) becomes

$$\frac{D\omega}{Dt} = \frac{\omega}{r} v + \nu \left[\frac{\partial^2 \omega}{\partial x^2} + \frac{\partial^2 \omega}{\partial r^2} + \frac{1}{r} \frac{\partial \omega}{\partial r} - \frac{\omega}{r^2} \right] \quad (2)$$

where v is the radial component of velocity. For an approximate formulation for large Reynolds number, it is not immediately justifiable to put $\nu = 0$. Rather, a limiting form for increasing Reynolds number indefinitely should be derived in a manner analogous to that for obtaining the boundary-layer momentum equations from the Navier-Stokes equations. The result depends upon the normalizing length scale chosen for the radial coordinates. The rotational flow layer is thick near the tail for reasons of mass conservation, particularly for bodies of low fineness ratio. If we assume that the appropriate radial length scale is not small in this region, unlike the situation for the upstream boundary layer, then the limiting form of the vorticity equation is

$$\frac{D\omega}{Dt} = \frac{\omega}{r} v \quad (3)$$

Although the shear stress mechanism is thus shown to have negligible effect on vorticity change for the aft rotational flow layer, a mathematical problem remains which supports the contention that a thin layer where shear stress is significant must exist next to the surface. The order of the governing equation has been reduced so that the condition of nonslip at the wall can no longer be enforced. It is therefore necessary to exclude a surface layer from the region where Eq. (3) is to be satisfied. This Note investigates the extent of the region for which vortex filament contraction is the dominant mechanism for vorticity change and for which Eq. (2) reduces to

$$\frac{D\omega}{Dt} - \frac{\omega}{r} v = r \frac{D}{Dt} \left(\frac{\omega}{r} \right) = 0 \quad (4)$$

Inviscid Rotational Flow Calculation

For incompressible inviscid axisymmetric flow, the ratio of vorticity to distance from the axis of symmetry is preserved along a streamline as indicated by Eq. (4), and we write

$$\omega / r = F(\psi) \quad (5)$$

The functional F for the stream function ψ is obtained from the known velocity field at the upstream border where fluid is flowing into the calculation region. If we express the vorticity in terms of the stream function, we obtain the governing equation for ψ:

$$-\frac{1}{r^2} \left(\psi_{xx} - \frac{1}{r} \psi_r + \psi_{rr} \right) = F(\psi) \quad (6)$$

Numerical techniques for solving this governing equation are available. However, an approximation is introduced which greatly simplifies the calculation. If local Cartesian axes are chosen with the x axis aligned with the flow, the second term in the defining equation for the vorticity

$$\omega = -\frac{\partial u}{\partial y} + \frac{\partial v}{\partial x} \quad (7)$$

can be neglected except where streamline curvature is large. Use of this approximation reduces Eq. (6) to the ordinary differential equation:

$$-\frac{d}{dy} \left(\frac{1}{r} \frac{d\psi}{dy} \right) = r F(\psi) \quad (8)$$

where y is the normal distance to the surface at the body station for which the equation is being applied. Its solution is equivalent to finding a velocity profile (u vs y) which satisfies

$$\omega = -\frac{du}{dy} = r F(\psi) \quad (9)$$

where

$$\psi = \int_0^{y'} ru \, dy \quad (10)$$

At a particular body station, a one-parameter family of velocity profiles can be constructed by a stepwise numerical procedure using finite-difference equations corresponding to Eqs. (9) and (10). The values for u and ψ are needed to start the calculation at either the upper or lower border of the calculation region. One of these is prescribed by the boundary condition, and the other is varied as the parameter for the family. The member of the family is then chosen so as to satisfy the boundary condition, a prescribed value for either ψ or u, at the other border of the calculation region.

The inverse of this procedure is applied at the upstream border of the calculation region to obtain the functional F appearing in Eq. (9). For this computation, u is known as a function of y, and ψ and ω are calculated according to Eqs. (9) and (10).

Treatment of the Surface Shear Stress Layer

The lower boundary condition for the calculation region is obtained by matching to a flow calculation for the adjacent surface layer where shear stress cannot be neglected. Given the velocity at the upper boundary of this layer, it is necessary to calculate the stream function at this boundary. Only the shape of the velocity profile is needed for the calculation. Fortunately, the solution for the calculation region is insensitive to the value for the stream function enforced at the lower border so that it is sufficiently accurate to assume any reasonable shape for the surface layer velocity profile. Test calculations showed little effect in changing n from 1 to 7 (see the next section) when a "$1/n$" power law velocity profile was assumed for the surface layer flow.

Sample Calculation Matched to an Experimental Upstream and Outer Flow

The flow was calculated about the aft 20% of a low fineness ratio body for which geometric definition and extensive velocity measurements are given by Patel and Lee.[5] The comparison between the calculated and measured velocity profile at the 94% body station shown in Fig. 1 typifies the good agreement obtained. For the calculation shown, the measured velocity profile at the 80% body station (also displayed on the figure) was used to obtain the functional F for Eq. (9), the measured velocity was used for the upper boundary condition, and the calculation region was extended down to $y/L = 0.00225$ (L = body length) where boundary conditions were matched to a surface flow layer approximated by a one-seventh power velocity profile. The calculation was not very sensitive to the choice for the height or the profile shape of this surface layer. Assuming a linear profile, for example, provides a solution nearly indistinguishable from that shown in Fig. 1 above $y/L = 0.004$.

The error from neglecting the change in vorticity imparted to a fluid element by shear stress increases as the element proceeds downstream. Nevertheless the difference between experiment and calculation is still small at the end of the body, as shown in Fig. 2. This result is remarkable since shear stress was "turned off" at the 80% body station for these calculations. The calculated profiles shown in Fig. 2 are two

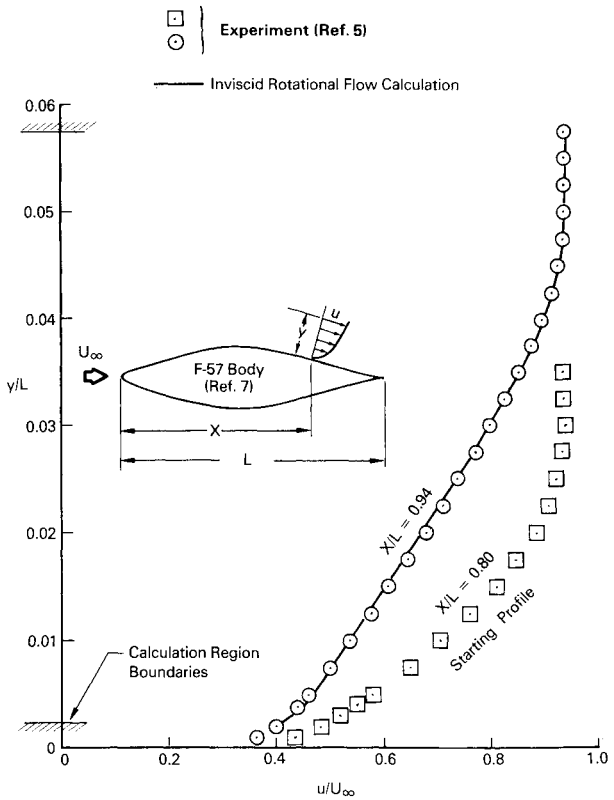

Fig. 1 The starting velocity profile at the upstream boundary, and the comparison of the experimental and calculated profiles at the 94% body station.

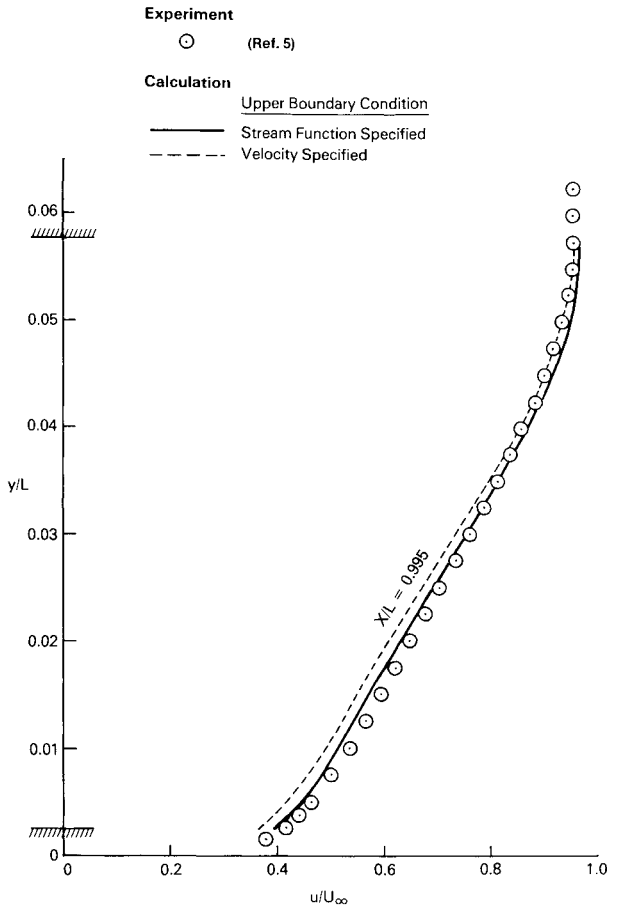

Fig. 2 Comparison of experiment with calculated velocity profiles at the 99.5% body station.

members of the one-parameter family of profiles which satisfy Eq. (9) and which match a one-seventh power velocity profile for a surface sublayer extending to $y/L = 0.0025$. One member satisfies the upper boundary condition for the velocity, and the other satisfies the upper boundary condition for the stream function, conditions obtained from the experimental measurements. For the 94% body station, these two different boundary conditions gave nearly indistinguishable solutions, and only one is shown in Fig. 1.

Summary and Conclusions

This study supports the hypothesis that viscous and Reynolds stresses in the tail region of a low fineness ratio body of revolution with an unseparated turbulent boundary layer do not provide the significant mechanism for vorticity change except in a thin surface sublayer. The dominant mechanism is the radial contraction of the material vortex ring filaments as they approach the tail. A simple calculation method based on this hypothesis and an approximate expression for the vorticity, plus a rudimentary account for the viscous surface layer provided excellent agreement with experimental measurements about a low fineness ratio body. Further investigation is needed to establish confidence in this simple treatment and to delineate the upstream extent and types of bodies for which it is applicable.

Acknowledgment

This work was supported by the Office of Naval Research under Contract N-00014-77-C-0364.

References

[1] Young, A. D., "The Calculation of the Total and Skin Friction Drags of Bodies of Revolution at Zero Incidence," Aeronautical Research Council, London, England, R & M 1874, 1939.

[2] Granville, P. S., "The Calculation of Viscous Drag of Bodies of Revolution," David Taylor Model Basin, Washington, D.C., Rept. 849, 1953.

[3] Patel, V. C. and Guven, O., "Importance of the Near Wake in Drag Prediction of Bodies of Revolution," *AIAA Journal*, Vol. 14, Aug. 1976, pp. 1132-1133.

[4] Melnik, R. E. and Chow, R., "Asymptotic Theory of Two-Dimensional Trailing Edge Flows," NASA Conference on *Aerodynamic Analysis Requiring Advanced Computors*, NASA SP 347 (also Grumman Research Dept. Rept. RE-510J), 1975.

[5] Patel, V. C. and Lee, Y. T., "Thick Axisymmetric Turbulent Boundary Layer and Near Wake of a Low-Drag Body of Revolution," Iowa Institute of Hydraulic Research (IIHR), The Univ. of Iowa, Rept. No. 210, Dec. 1977.